

Effect of the mixing of s-wave and chiral p-wave pairings on electrical shot noise properties of normal metal/superconductor tunnel junctions

Yu-Chen Hu(胡雨辰) and Liang-Bin Hu(胡梁宾)

Citation: Chin. Phys. B, 2024, 33 (**7**): 077202. DOI: 10.1088/1674-1056/ad498a
Journal homepage: http://cpb.iphy.ac.cn; http://iopscience.iop.org/cpb

What follows is a list of articles you may be interested in

Anomalous Josephson effect between d-wave superconductors through a two-dimensional electron gas with both Rashba spin-orbit coupling and Zeeman splitting

Bin-Hao Du(杜彬豪), Mou Yang(杨谋), and Liang-Bin Hu(胡梁宾)
Chin. Phys. B, 2023, 32 (**7**): 077201. DOI: 10.1088/1674-1056/accc7f

Influence of Rashba spin-orbit coupling on Josephson effect in triplet superconductor/two-dimensional semiconductor/triplet superconductor junctions

Bin-Hao Du(杜彬豪), Man-Ni Chen(陈嫚妮), and Liang-Bin Hu(胡梁宾)
Chin. Phys. B, 2022, 31 (**7**): 077201. DOI: 10.1088/1674-1056/ac587e

Effects of interface bound states on the shot noise in normal metal-low-dimensional Rashba semiconductor tunnel junctions with induced s-wave pairing potential

Wen-Xiang Chen(陈文祥), Rui-Qiang Wang(王瑞强), Liang-Bin Hu(胡梁宾)
Chin. Phys. B, 2019, 28 (**5**): 057201. DOI: 10.1088/1674-1056/28/5/057201

Observation of nonconservation characteristics of radio frequency noise mechanism of 40-nm n-MOSFET

Jun Wang(王军), Xiao-Mei Peng(彭小梅), Zhi-Jun Liu(刘志军), Lin Wang(王林), Zhen Luo(罗震), Dan-Dan Wang(王丹丹)
Chin. Phys. B, 2018, 27 (**2**): 027201. DOI: 10.1088/1674-1056/27/2/027201

Electronic band gap and transport in graphene superlattice with a Gaussian profile potential voltage

Zhang Yu-Ping (张玉萍), Yin Yi-Heng (尹贻恒), Lü Huan-Huan (吕欢欢), Zhang Hui-Yun (张会云)
Chin. Phys. B, 2014, 23 (**2**): 027202. DOI: 10.1088/1674-1056/23/2/027202

Effect of the mixing of s-wave and chiral p-wave pairings on electrical shot noise properties of normal metal/superconductor tunnel junctions

Yu-Chen Hu(胡雨辰) and Liang-Bin Hu(胡梁宾)†

Guangdong Provincial Key Laboratory of Quantum Engineering and Quantum Materials, School of Physics, South China Normal University, Guangzhou 510631, *China*

(Received 28 December 2023; revised manuscript received 20 April 2024; accepted manuscript online 10 May 2024)

We study theoretically the electrical shot noise properties of tunnel junctions between a normal metal and a superconductor with the mixture of singlet s-wave and chiral triplet p-wave pairing due to broken inversion symmetry. We investigate how the shot noise properties vary as the relative amplitude between the two parity components in the pairing potential is changed. It is demonstrated that some characteristics of the electrical shot noise properties of such tunnel junctions may depend sensitively on the relative amplitude between the two parity components in the pairing potential, and some significant changes may occur in the electrical shot noise properties when the relative amplitude between the two parity components is varied from the singlet s-wave pairing dominated regime to the chiral triplet p-wave pairing dominated regime. In the chiral triplet p-wave pairing dominated regime, the ratio of noise power to electric current is close to $2e$ both in the in-gap and in the out-gap region. In the singlet s-wave pairing dominated regime, the value of this ratio is close to $4e$ in the inner gap region but may reduce to about $2e$ in the outer gap region as the relative amplitude of the chiral triplet pairing component is increased. The variations of the differential shot noise with the bias voltage also exhibit some significantly different features in different regimes. Such different features can serve as useful diagnostic tools for the determination of the relative magnitude of the two parity components in the pairing potential.

Keywords: normal metal/superconductor tunnel junctions, shot noise, mixing of s-wave and chiral p-wave pairing, spin–orbit coupling

PACS: 72.10.Bg, 72.25.Dc, 72.25.Ba, 72.15.–v **DOI:** 10.1088/1674-1056/ad498a

1. Introduction

The parity symmetry of Cooper pairs is a fundamental property of a superconducting phase. If there is no coupling between the electrons' spin and orbital degrees of freedom, the wave function of a Cooper pair can be decomposed into the product of a spin part and an orbital part, then two types of parity symmetry can be classified for pairing states, namely spin-singlet pairing with orbital even-parity and spin-triplet pairing with orbital odd-parity.[1,2] This classification is valid in the absence of spin–orbit interaction but becomes invalid in the presence of strong spin–orbit coupling. For example, in some non-centrosymmetric superconductors[3–7] and in some proximity-induced superconducting phases developed in some low-dimensional semiconductor nanostructures[8–15] or topological insulator surfaces,[16–23] the broken inversion symmetry may not only lead to strong spin–orbit interaction but also cause the mixing of singlet s-wave and chiral triplet p-wave pairing. It is expected that some peculiar properties may occur due to the mixing of singlet and chiral triplet pairing, such as topologically protected zero-energy bound modes,[16–23] spin-polarized dissipationless charge current,[24,25] topological spin current,[26,27] magnetoelectric effects,[28,29] *etc*.

When both singlet and chiral triplet pairing component coexist in the pairing potential, the determination of the relative magnitude of the two parity components is a fundamental issue since some properties of a superconducting phase may depend sensitively on it. Various schemes have been proposed for testing the structure of the parity-mixed pairing states.[30–36] Most of these schemes are based on the measurement of electrical transport properties of various types of junctions consisting of such superconducting phases, *e.g.*, through the measurement of the tunneling spectroscopy. In a single-barrier tunnel junction between a normal metal and such a superconductor, the observation of a zero-bias anomaly in quasiparticle tunneling spectroscopy of certain directions is widely believed to be an indication of the presence of helical edge state of topologically non-trivial phase with dominant spin-triplet odd-parity pairing.[31] In addition, the helical states would carry spin currents which would be another indication for the topologically non-trivial state with dominant spin-triplet odd-parity pairing.[32] In a double-barrier tunnel junction consisting of such a superconductor sandwiched by two spin-polarized normal metals, some characteristics of crossed Andreev reflection between two interfaces can also serve as a diagnostic tool for the relative ratio of the singlet and the triplet component in the pairing potential.[33] Some other possible schemes were also proposed based on the measurement of some other types of electrical transport properties which

†Corresponding author. E-mail: lbhu26@126.com

© 2024 Chinese Physical Society and IOP Publishing Ltd

may depend sensitively on the relative amplitude between the two parity components in the pairing potential.[34–36]

In this paper we study theoretically the possibility of utilizing the measurement of electrical shot noise properties in tunnel junctions as a probe of the relative magnitude of singlet s-wave and chiral triplet p-wave pairing component in a superconducting phase with mixed parity due to broken inversion symmetry. The electrical shot noise originates from the time-dependent fluctuation of the electric current in electrical transport due to the discreteness of the charge of the carriers and remains as the only source of electrical noise in the zero-temperature limit. It is well known that the shot noise measurements in the zero-temperature limit can provide some valuable information on the transport process in a tunnel junction, which is not available through usual conductance measurements.[37–44] For instance, in tunnel junctions between normal metallic conductors with the carriers charged e, the process of electrical conductance can be modeled by a Poisson process in the absence of correlations among the carriers, then the ratio of noise power to electric current will equal to $2e$ in the zero-temperature limit for small bias voltage.[37] In contrast, in a low transmission tunnel junction between a normal metal and a conventional s-wave superconductor with singlet pairing, the value of this ratio will be doubled for small bias voltage due to the transport of Cooper pairs charged $2e$, so some useful information on the charge and statistics of quasiparticles may be revealed through the measurement of electrical shot noise properties.[37–40] But it should be noted that, if singlet and chiral triplet pairing coexist in the superconducting region of a tunnel junction, the situations become somewhat different and the results may change substantially due to the Pauli repulsion between electrons with the same spin projections. Moreover, helical edge state may occur at the junction interface if the effect of chiral triplet pairing exceeds that of singlet pairing, which may also affect substantially the electrical shot noise properties of such a tunnel junction. In this paper, based on the Bogoliubov–de Gennes (BdG) equation and the extended Landauer–Büttiker scattering theory,[45] we investigate theoretically the characteristics of the electrical shot noise properties of tunnel junctions between a normal metal and such a superconductor where strong Rashba spin–orbit coupling and the mixture of singlet s-wave and chiral triplet p-wave pairing coexist. We investigate in some detail how the shot noise properties vary as the relative amplitude between the singlet s-wave and the chiral triplet p-wave component in the pairing potential is changed. It is demonstrated that some significant changes may occur in the electrical shot noise properties as the relative amplitude between the two parity components is varied. For instance, in the chiral triplet p-wave pairing dominated regime, the ratio of noise power to electric current is close to $2e$ both in the in-gap and in the out-gap region. In contrast, in the singlet s-wave pairing dominated regime, the value of this ratio is close to $4e$ in the inner gap region but may reduce to about $2e$ in the outer gap region as the relative amplitude of the chiral triplet pairing component is increased. The variations of the differential shot noise with the bias voltage also exhibit some significant differences in different regimes of the relative amplitude of the two parity components. The observation of such different features in the electrical shot noise properties can serve as useful diagnostic tools in the determination of the relative amplitude between the two parity components, in complement to usual diagnostic tools based on conductance measurements.

The paper is organized as follows. In Section 2 we describe the theoretical model for the considered structure and introduce the theoretical formulation for the calculation of the electrical shot noise. In Section 3 we calculate numerically the electrical shot noise and investigate in some detail what changes may occur in the electrical shot noise properties as the relative magnitude of the two parity components in the pairing potential is varied. A summary is given in Section 4.

2. Model and formulation

We consider a single-barrier planar tunnel junction lying in the x–y plane, where on the side of $x<0$ is a normal metal and on the side of $x>0$ is a superconductor where the mixture of singlet s-wave and chiral triplet p-wave pairing and strong Rashba spin–orbit coupling coexist due to broken inversion symmetry. The junction interface is located at $x=0$ and is assumed to be perfectly flat and extends infinitely along the y direction. The voltage bias is along the x direction. In the normal metal region ($x<0$), the electronic state is described by the following single-particle effective Hamiltonian: $H_0(\boldsymbol{k})=\hbar^2\boldsymbol{k}^2/(2m)-\mu$, where m is the electron effective mass, μ is the chemical potential, and $\boldsymbol{k}=(k_x,k_y)$ is the two-dimensional wave vector. In the superconducting region ($x>0$), the quasiparticle excitation is described by the following BdG Hamiltonian:[2,3,6]

$$H(\boldsymbol{k})=\begin{bmatrix}\xi_{\boldsymbol{k}}+\lambda(k_y\sigma_x-k_x\sigma_y) & \hat{\Delta}(\boldsymbol{k})\\ -\hat{\Delta}^*(-\boldsymbol{k}) & -\xi_{\boldsymbol{k}}+\lambda(k_y\sigma_x+k_x\sigma_y)\end{bmatrix}, \quad (1)$$

where $\hat{\Delta}(\boldsymbol{k})$ is the pairing potential matrix, $\xi_{\boldsymbol{k}}=\hbar^2\boldsymbol{k}^2/(2m)-\mu$ is the kinetic energy relative to the chemical potential μ, $\sigma_{x,y,z}$ denotes the Pauli matrices in spin space, and λ denotes the strength of Rashba spin–orbit coupling. For simplicity, we assume the same electron effective mass m and chemical potential μ on both side of $x<0$ and $x>0$.

In the presence of both singlet s-wave and chiral triplet p-wave pairing, the pairing potential $\hat{\Delta}(\boldsymbol{k})$ can be written as $\hat{\Delta}(\boldsymbol{k})=[\boldsymbol{d}(\boldsymbol{k})\cdot\hat{\boldsymbol{\sigma}}]\mathrm{i}\sigma_y+\mathrm{i}\Delta_{\mathrm{S}}(\boldsymbol{k})\sigma_y$, where $\Delta_{\mathrm{S}}(\boldsymbol{k})$ is the singlet component and $\boldsymbol{d}(\boldsymbol{k})$ the triplet component. We assume that

the triplet component $\boldsymbol{d}(\boldsymbol{k})$ is aligned with the spin–orbit field, then the triplet component can be written as[7]

$$\boldsymbol{d}(\boldsymbol{k}) = \Delta_{\rm P}(\boldsymbol{k})\frac{\hat{x}k_y - \hat{y}k_x}{k}, \tag{2}$$

where $\Delta_{\rm P}(\boldsymbol{k})$ is the amplitude of the triplet pairing component, $\hat{x}$ and $\hat{y}$ denote the unit vectors along the x and y directions, respectively. In the following we consider only the mean-field value of the amplitude $\Delta_{\rm S}(\boldsymbol{k})$ and $\Delta_{\rm P}(\boldsymbol{k})$ and neglect the dependences on wave vector $\boldsymbol{k}$, i.e., setting $\Delta_{\rm S}(\boldsymbol{k}) = \Delta_{\rm S}$ and $\Delta_{\rm P}(\boldsymbol{k}) = \Delta_{\rm P}$, with $\Delta_{\rm S}, \Delta_{\rm P} \geqslant 0$. In Nambu-spin space, the effective Hamiltonian describing the low energy excitation in the entire junction area can then be written in the following 4×4 matrix form:

$$H = \begin{bmatrix} \xi_{\boldsymbol{k}} + U(x) & {\rm i}\lambda k_-\Theta(x) & -{\rm i}\Delta_{\rm P}{\rm e}^{-{\rm i}\theta}\Theta(x) & \Delta_{\rm S}\Theta(x) \\ -{\rm i}\lambda k_+ & \xi_{\boldsymbol{k}} + U(x) & -\Delta_{\rm S}\Theta(x) & -{\rm i}\Delta_{\rm P}{\rm e}^{{\rm i}\theta}\Theta(x) \\ {\rm i}\Delta_{\rm P}{\rm e}^{{\rm i}\theta}\Theta(x) & -\Delta_{\rm S}\Theta(x) & -\xi_{\boldsymbol{k}} - U(x) & -{\rm i}\lambda k_+\Theta(x) \\ \Delta_{\rm S}\Theta(x) & {\rm i}\Delta_{\rm P}{\rm e}^{-{\rm i}\theta}\Theta(x) & {\rm i}\lambda k_-\Theta(x) & -\xi_{\boldsymbol{k}} - U(x) \end{bmatrix}. \tag{3}$$

Here θ represents the angle between the direction of quasiparticles' motion and the x axis, $k_\pm = k_x \pm {\rm i}k_y = k{\rm e}^{\pm{\rm i}\theta}$, $\Theta(x)$ is the Heaviside step function, and $U(x)$ is the interface barrier potential. For simplicity, we assume a δ-type barrier potential $U(x) = U_0\delta(x)$ at the junction interface, with U_0 being the barrier strength.

Since translational invariance is assumed along the y direction in the junction, the solutions of the BdG equation can be described by the general ansatz $\psi(x){\rm e}^{{\rm i}k_y y}$, where k_y is the transverse component of the wave vector of a quasiparticle state and $\psi(x)$ is the longitudinal solution of the BdG Hamiltonian for the effective one-dimensional scattering problem along the x direction, which can be constructed from the eigensolutions of the BdG Hamiltonian in each different regions of the junction. Then for an electron incident from the normal metal side with a transverse wave vector component k_y and excitation energy E and spin σ, the scattering state in the normal metal region ($x<0$) can be expressed as

$$\begin{aligned}\Psi(x) \;=\; & {\rm e}^{{\rm i}k_y y}[{\rm e}^{{\rm i}k_x^{(\rm e)}x}|\sigma\rangle_{\rm e} + a_{\sigma\sigma}{\rm e}^{{\rm i}k_x^{(\rm h)}x}|\sigma\rangle_{\rm h} \\ & + a_{\sigma\bar{\sigma}}{\rm e}^{{\rm i}k_x^{(\rm h)}x}|\bar{\sigma}\rangle_{\rm h} + b_{\sigma\sigma}{\rm e}^{-{\rm i}k_x^{(\rm e)}x}|\sigma\rangle_{\rm e} \\ & + b_{\sigma\bar{\sigma}}{\rm e}^{-{\rm i}k_x^{(\rm e)}x}|\bar{\sigma}\rangle_{\rm e}]. \end{aligned} \tag{4}$$

Here $|\sigma\rangle_{\rm e(h)}$ represent the spinor functions of electrons (e) or holes (h) with spin-up ($\sigma = +$) or spin-down ($\sigma = -$) and $|\bar{\sigma}\rangle_{\rm e(h)}$ ($\bar{\sigma} = -\sigma$) the spinor functions of the spin-flip states, which are defined respectively in the following: $|+\rangle_{\rm e} = [1,0,0,0]^{\rm T}$, $|-\rangle_{\rm e} = [0,1,0,0]^{\rm T}$, $|+\rangle_{\rm h} = [0,0,1,0]^{\rm T}$, and $|-\rangle_{\rm h} = [0,0,0,1]^{\rm T}$. The $a_{\sigma\sigma}$ is the spin-conserving Andreev reflection coefficient and $a_{\sigma\bar{\sigma}}$ is the spin-flip Andreev reflection coefficient. The $b_{\sigma\sigma}$ is the spin-conserving normal reflection coefficient and $b_{\sigma\bar{\sigma}}$ is the spin-flip normal reflection coefficient. $k_x^{(\rm e,h)}$ are the longitudinal wave vector components of quasiparticles and are determined by the transverse wave vector component k_y and excitation energy E as follows: $k_x^{(\rm e)} = \sqrt{(2m/\hbar^2)(\mu+E) - k_y^2}$, $k_x^{(\rm h)} = \sqrt{(2m/\hbar^2)(\mu-E) - k_y^2}$.

In the superconducting region ($x>0$), the scattering state can be expressed as the linear combination of two electron-like and two hole-like right-moving eigenstates of the BdG Hamiltonian. Defining $\gamma = {\rm sgn}(\Delta_{\rm P} - \Delta_{\rm S})$, the wavefunction of the scattering state in the superconducting region can then be expressed as

$$\begin{aligned}\psi(x) \;=\; & c_1\begin{bmatrix} u_1 \\ -{\rm i}u_1/g_1 \\ {\rm i}v_1/g_1 \\ v_1 \end{bmatrix}\exp({\rm i}q_{1x}^{\rm e}x + {\rm i}k_y y) \\ & + c_2\begin{bmatrix} u_2 \\ {\rm i}u_2/g_2 \\ {\rm i}\gamma v_2/g_2 \\ -\gamma v_2 \end{bmatrix}\exp({\rm i}q_{2x}^{\rm e}x + {\rm i}k_y y) \\ & + d_1\begin{bmatrix} v_1 \\ -{\rm i}v_1/\tilde{g}_1 \\ {\rm i}u_1/\tilde{g}_1 \\ u_1 \end{bmatrix}\exp(-{\rm i}q_{1x}^{\rm h}x + {\rm i}k_y y) \\ & + d_2\begin{bmatrix} v_2 \\ {\rm i}v_2/\tilde{g}_2 \\ {\rm i}\gamma u_2/\tilde{g}_2 \\ -\gamma u_2 \end{bmatrix}\exp(-{\rm i}q_{2x}^{\rm h}x + {\rm i}k_y y), \end{aligned} \tag{5}$$

where the first two terms on the right side of the equation represent two electronlike right-moving propagating modes with the longitudinal wave vector components $q_{1(2)x}^{\rm e}$, the last two terms represent two holelike right-moving propagating modes with the longitudinal wave vector components $q_{1(2)x}^{\rm h}$, $c_{1(2)}$ and $d_{1(2)}$ are the corresponding scattering coefficients. The coherence factors $u_{1(2)}$ and $v_{1(2)}$ are functions of the quasiparticle excitation energy E and are defined respectively by

$$u_{1(2)} \;=\; \sqrt{\frac{1}{2}\left(1 + \frac{\sqrt{E^2 - \Delta_{1(2)}^2}}{E}\right)}, \tag{6}$$

$$v_{1(2)} \;=\; \sqrt{\frac{1}{2}\left(1 - \frac{\sqrt{E^2 - \Delta_{1(2)}^2}}{E}\right)}, \tag{7}$$

where $\Delta_1 = \Delta_{\rm P} + \Delta_{\rm S}$ and $\Delta_2 = |\Delta_{\rm S} - \Delta_{\rm P}|$. The longitudinal wave vector components $q_{1(2)x}^{\rm e(h)}$ and the factors $g_{1(2)}$ and $\tilde{g}_{1(2)}$

are all functions of the quasiparticle excitation energy E and the transverse wave vector component k_y. Among them, $q^{\mathrm{e(h)}}_{1(2)x}$ are related to E and k_y by the following dispersion relation: $E=\sqrt{(\xi_{\boldsymbol{k}}\pm\lambda|\boldsymbol{k}|)^2+\Delta_{\mathrm{P}}^2+\Delta_{\mathrm{S}}^2}$, with $\boldsymbol{k}=(q^{\mathrm{e(h)}}_{1(2)x},k_y)$. From this dispersion relation, one gets

$$q^{\mathrm{e}}_{1(2)x}=k^{\mathrm{e}}_{1(2)x}+\frac{k_{1(2)}}{k^{\mathrm{e}}_{1(2)x}}\sqrt{\frac{E^2-\Delta^2_{1(2)}}{\lambda^2+2\hbar^2\mu/m}}, \tag{8}$$

$$q^{\mathrm{h}}_{1(2)x}=k^{\mathrm{h}}_{1(2)x}-\frac{k_{1(2)}}{k^{\mathrm{h}}_{1(2)x}}\sqrt{\frac{E^2-\Delta^2_{1(2)}}{\lambda^2+2\hbar^2\mu/m}}, \tag{9}$$

where $k^{\mathrm{e}}_{1(2)x}=\sqrt{k^2_{1(2)}-k_y^2}$ for both $|k_y|<k_{1(2)}$ and $|k_y|>k_{1(2)}$, $k^{\mathrm{h}}_{1(2)x}=\sqrt{k^2_{1(2)}-k_y^2}$ for $|k_y|<k_{1(2)}$ and $k^{\mathrm{h}}_{1(2)x}=-\sqrt{k^2_{1(2)}-k_y^2}$ for $|k_y|>k_{1(2)}$, with

$$k_1=-\frac{m\lambda}{\hbar^2}+\sqrt{\left(\frac{m\lambda}{\hbar^2}\right)^2+\frac{2m\mu}{\hbar^2}},$$

$$k_2=\frac{m\lambda}{\hbar^2}+\sqrt{\left(\frac{m\lambda}{\hbar^2}\right)^2+\frac{2m\mu}{\hbar^2}}.$$

After $q^{\mathrm{e(h)}}_{1(2)x}$ are obtained as the functions of E and k_y, the factors $g_{1(2)}$ and $\tilde{g}_{1(2)}$ as the functions of E and k_y can be obtained as follows: $g_{1(2)}=(k^{\mathrm{e}}_{1(2)x}-\mathrm{i}k_y)/k_{1(2)}$, $\tilde{g}_{1(2)}=-(k^{\mathrm{h}}_{1(2)x}+\mathrm{i}k_y)/k_{1(2)}$.

All the scattering coefficients in Eqs. (4) and (5) can be determined by the boundary conditions at the junction interface at $x=0$, which read

$$\Psi|_{x=0^-}=\Psi|_{x=0^+}, \tag{10}$$

$$\hat{V}_x^{(\mathrm{N})}\Psi|_{x=0^-}=\hat{V}_x^{(\mathrm{S})}\Psi|_{x=0^+}-\frac{\hbar}{m\mathrm{i}}\frac{2mU_0}{\hbar^2}(\sigma_0\otimes\tau_z)\Psi|_{x=0^+}, \tag{11}$$

where $\hat{V}_x^{(\mathrm{N})}$ is the x component of the velocity operator in the normal metal region and $\hat{V}_x^{(\mathrm{S})}$ the x component of the velocity operator in the superconducting region, σ_0 is the unit matrix in spin space and τ_z the Pauli matrix in particle–hole space. By solving Eqs. (10) and (11), for an incident electron with excitation energy E and incident angle θ (defined by $k_y=k\sin\theta$), the normal and the Andreev reflection coefficients $b_{\sigma\sigma'}$ and $a_{\sigma\sigma'}$ in Eq. (4) can be obtained, which are functions of both E and θ. In the following we use $R^{\mathrm{e}}_{\sigma\sigma'}$ to denote the normal reflection probabilities of an incident electron with spin σ reflected to an electron with spin σ', and use $R^{\mathrm{h}}_{\sigma\sigma'}$ to denote the Andreev reflection probabilities of an incident electron with spin σ reflected to a hole with spin σ'. In terms of the normal and the Andreev reflection coefficients $b_{\sigma\sigma'}(E,\theta)$ and $a_{\sigma\sigma'}(E,\theta)$, the normal and the Andreev reflection probabilities $R^{\mathrm{e}}_{\sigma\sigma'}$ and $R^{\mathrm{h}}_{\sigma\sigma'}$ of an incident electron with excitation energy E and spin σ and incident angle θ are given by

$$R^{\mathrm{e}}_{\sigma\sigma'}=|b_{\sigma\sigma'}(E,\theta)|^2,\quad R^{\mathrm{h}}_{\sigma\sigma'}=\frac{k_x^{(\mathrm{h})}}{k_x^{(\mathrm{e})}}|a_{\sigma\sigma'}(E,\theta)|^2, \tag{12}$$

which are also functions of both E and θ.

After the normal and the Andreev reflection probabilities are obtained, the average electric current and the fluctuation around the average electric current (i.e., the electrical shot noise) can be obtained following the extended Landauer–Büttiker scattering theory.[37,38,45] In the zero-temperature limit, the average electric current at a bias voltage V is given by

$$I=\frac{1}{e}\int_0^{eV}G(E)\,\mathrm{d}E, \tag{13}$$

where $G(E)$ is the differential tunneling conductance at zero-temperature, which can be expressed as an integration over the incident angle θ as follows:

$$\begin{aligned}G(E)=\frac{e^2}{2h}\sum_\sigma\int_{-\pi/2}^{\pi/2}\big[1+R^{\mathrm{h}}_{\sigma\sigma}+R^{\mathrm{h}}_{\sigma\bar{\sigma}}\\-R^{\mathrm{e}}_{\sigma\sigma}-R^{\mathrm{e}}_{\sigma\bar{\sigma}}\big]\cos\theta\,\mathrm{d}\theta.\end{aligned} \tag{14}$$

In the zero-temperature limit, the shot-noise power at a bias voltage V is given by

$$P=\frac{1}{e}\int_0^{eV}S(E)\,\mathrm{d}E, \tag{15}$$

where $S(E)$ is the differential shot noise at zero-temperature, which can be expressed as an integration over the incident angle θ as follows:

$$S(E)=\frac{e^3}{h}\sum_\sigma\int_{-\pi/2}^{\pi/2}s_\sigma(E,\theta)\cos\theta\,\mathrm{d}\theta, \tag{16}$$

where $s_\sigma(E,\theta)$ is given by the normal and the Andreev reflection probabilities as follows:

$$\begin{aligned}s_\sigma(E,\theta)=&R^{\mathrm{e}}_{\sigma\sigma}(1-R^{\mathrm{e}}_{\sigma\sigma})+R^{\mathrm{e}}_{\sigma\bar{\sigma}}(1-R^{\mathrm{e}}_{\sigma\bar{\sigma}})\\&+R^{\mathrm{h}}_{\sigma\sigma}(1-R^{\mathrm{h}}_{\sigma\sigma})+R^{\mathrm{h}}_{\sigma\bar{\sigma}}(1-R^{\mathrm{h}}_{\sigma\bar{\sigma}})\\&+2R^{\mathrm{e}}_{\sigma\sigma}R^{\mathrm{e}}_{\sigma\bar{\sigma}}+2R^{\mathrm{h}}_{\sigma\sigma}R^{\mathrm{h}}_{\sigma\bar{\sigma}}\\&+2(R^{\mathrm{e}}_{\sigma\sigma}+R^{\mathrm{e}}_{\sigma\bar{\sigma}})(R^{\mathrm{h}}_{\sigma\sigma}+R^{\mathrm{h}}_{\sigma\bar{\sigma}}).\end{aligned} \tag{17}$$

3. Results and discussion

We now present the numerical results obtained based on the formulation outlined above, focusing on the variations of the shot noise properties with the changes of the relative amplitude between the singlet and the chiral triplet component of the pairing potential. Dimensionless parameters are used below. The barrier strength is defined by a dimensionless parameter $Z\equiv 2mU_0/(\hbar^2k_{\mathrm{F}})$, with k_{F} being the Fermi wave number. The strength of RSOI is defined by a dimensionless parameter $\alpha=2m\lambda/(\hbar^2k_{\mathrm{F}})$. The magnitude of the pairing potential is measured by chemical potential μ. We fix $\Delta\equiv\Delta_{\mathrm{S}}+\Delta_{\mathrm{P}}=0.001\mu$ in the calculations but vary the relative amplitude between Δ_{S} and Δ_{P}.

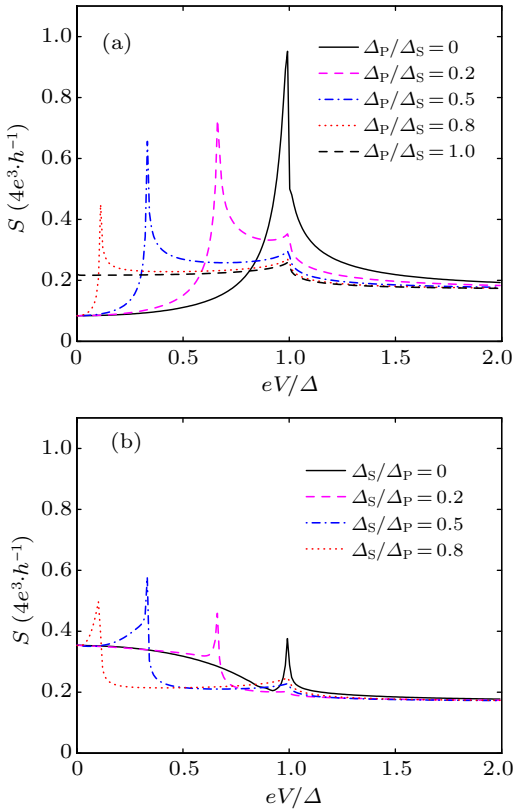


Fig. 1. The variation of the differential shot noise with the bias voltage for several different values of the relative amplitude between Δ_S and Δ_P. The results shown in panels (a) and (b) correspond to the cases $\Delta_S/\Delta_P \geq 1$ and $\Delta_S/\Delta_P < 1$ respectively. The value of Δ_P/Δ_S (or Δ_S/Δ_P) is shown in the insets in the figures. The other parameters are: $\Delta = 0.001\mu$, $Z = 3$, $\alpha = 0.5$.

In Fig. 1 we show the differential shot noise S (in units of $4e^3/h$) as a function of the bias voltage V (in units of Δ/e) for several different values of the relative amplitude between Δ_S and Δ_P. We consider three different regimes of interest: $\Delta_S > \Delta_P$, $\Delta_S = \Delta_P$, and $\Delta_S < \Delta_P$. The results shown in Figs. 1(a) and 1(b) correspond to the cases with $\Delta_S \geq \Delta_P$ and the cases with $\Delta_S < \Delta_P$, respectively. From the results shown in Figs. 1(a) and 1(b), we can see that the differential shot noise spectrums exhibit some significant differences in the three different regimes. Figure 1(a) shows that, if $\Delta_P = 0$ (the pairing is purely singlet), the differential shot noise spectrum exhibits only a single sharp peak at the bias voltage $V = \Delta/e$. As the bias voltage is increased, the differential shot noise S increases monotonically in the in-gap region of $V < \Delta/e$ and decreases monotonically in the out-gap region of $V > \Delta/e$. In contrast, if $\Delta_P \neq 0$ but $\Delta_P/\Delta_S < 1$ (the singlet pairing is dominant), the differential shot noise spectrum exhibits two peaks. A sharp peak appears in the in-gap region of $V < \Delta/e$ and a small peak appears at $V = \Delta/e$. Compared with the peak in the in-gap region, the height of the peak at $V = \Delta/e$ is greatly suppressed and decreases slowly with the increase of Δ_P/Δ_S. For the peak in the in-gap region, both its height and its position depend sensitively on the relative amplitude between Δ_P and Δ_S. As Δ_P/Δ_S is increased, the peak height decreases substantially and the peak position shifts gradually toward the direction of zero-bias voltage. When $\Delta_P = \Delta_S$, the peak in the in-gap region vanishes and the value of S increases sharply in the vicinity of zero-bias voltage. In this case, the variation of S with the bias voltage becomes rather smooth and rather small both in the in-gap region and in the out-gap region.

If the triplet component is dominant in the pairing potential ($\Delta_P > \Delta_S$), helical Andreev bound state will be formed at the junction interface[6,31,32] and the effect of the Pauli repulsion also becomes much substantial. As a result, the characteristics of the variation of the shot noise with the bias voltage may become significantly different from that shown in Fig. 1(a). This fact can be seen from the results shown in Fig. 1(b). From Fig. 1(b) we can see that, when $\Delta_S/\Delta_P = 0$ (the pairing is purely triplet), the differential shot noise spectrum also exhibits a single sharp peak at $V = \Delta/e$, but in the in-gap region of $V < \Delta/e$, the variation of S with the bias voltage is non-monotonic and significantly different from the singlet pairing dominated cases shown in Fig. 1(a). As the bias voltage is increased from zero, the value of S first decreases monotonically and smoothly with the increase of V, and then turns to increase sharply as V approaches Δ/e. When $\Delta_S/\Delta_P \neq 0$, the position of the sharp peak shifts into the in-gap region. On the low bias voltage side of the sharp peak in the in-gap region, the value of S first decreases monotonically and smoothly with the increase of V and then turns to increase sharply as V approaches the peak position, unlike the singlet pairing dominated cases shown in Fig. 1(a). A small and smooth peak may still occur at $V = \Delta/e$, but the height is greatly suppressed. As the value of Δ_S/Δ_P is increased, the position of the peak in the in-gap region shifts gradually toward the direction of zero-bias voltage. When Δ_S gets close to Δ_P, the peak in the in-gap region vanishes, and the value of S drops sharply in the vicinity of zero-bias voltage, recovering the corresponding result shown in Fig. 1(a) for the $\Delta_P = \Delta_S$ case.

Another important quantity characterizing the shot noise properties of a single-barrier normal metal/superconductor tunnel junction is the ratio of noise power (P) to electric current (I). In Fig. 2 we show the ratio P/I (in unit of $2e$) as a function of the bias voltage for several different values of the relative amplitude between Δ_S and Δ_P. Panels (a) and (b) in Fig. 2 correspond to the cases with $\Delta_S \geq \Delta_P$ and the cases with $\Delta_S < \Delta_P$, respectively. From the results shown in panels (a) and (b) in Fig. 2, we can see that the variations of the ratio P/I with the bias voltage also exhibit some qualitatively different features in the three different regimes of $\Delta_S > \Delta_P$, $\Delta_S = \Delta_P$, and $\Delta_S < \Delta_P$. Figure 2(a) shows that, when $\Delta_P/\Delta_S = 0$ (the pairing is purely singlet), the change curve of the ratio P/I

with the bias voltage has a plateau area in the in-gap region of $V < \Delta/e$. Within the plateau area, the value of P/I is about $4e$ and is little changed as the bias voltage is varied, indicating that the electric current is carried mainly by Cooper pairs in the in-gap region. In the out-gap region of $V > \Delta/e$, the value of P/I reduces rapidly to about $2e$ (the classical Schottky value) as the bias voltage is increased, indicating that the electric current is carried mainly by single electrons in the out-gap region. When $\Delta_P \neq 0$ but $\Delta_P/\Delta_S < 1$, the plateau area in the change curve of P/I with the bias voltage still exists in the inner gap region, but the width of the plateau area reduces substantially with the increase of Δ_P/Δ_S. The value of P/I is still about $4e$ in the plateau area. In the outer gap region beyond the plateau area, the value of P/I is intermediate between $4e$ and $2e$, indicating that the electric current is carried partly by Cooper pairs and partly by single electrons in this bias voltage region. When $\Delta_P/\Delta_S = 1$, the plateau area vanishes and the change curve becomes nearly flat, with the value of P/I close to $2e$ in the whole bias voltage region. Compared with the $\Delta_S > \Delta_P$ cases shown in Fig. 2(a), from Fig. 2(b) we can see that the variation of P/I with the bias voltage is rather small and smooth overall in the triplet pairing dominated cases. The value of P/I is slightly smaller than $2e$ in the vicinity of zero-bias voltage,

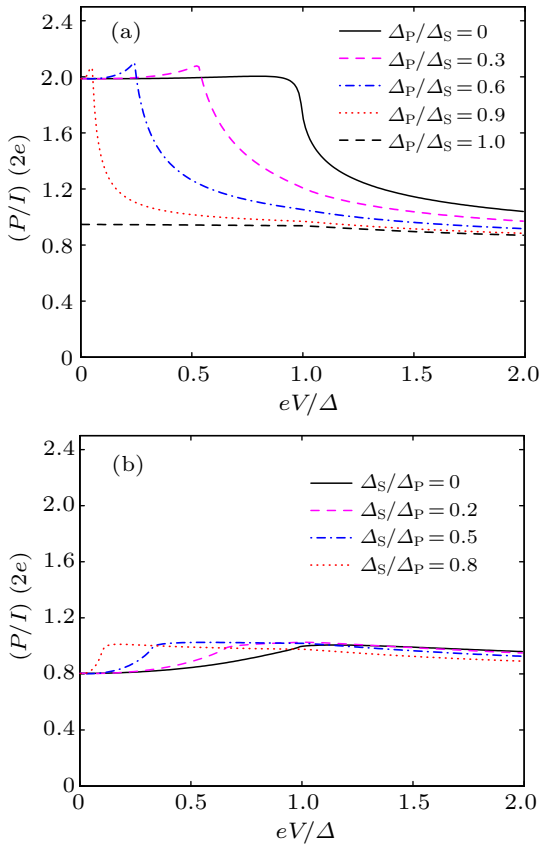


Fig. 2. The variation of the ratio of noise power to electric current with the bias voltage for several different values of the relative amplitude between Δ_S and Δ_P. The results shown in panels (a) and (b) correspond to the cases $\Delta_S/\Delta_P \geq 1$ and $\Delta_S/\Delta_P < 1$ respectively. The value of Δ_P/Δ_S (or Δ_S/Δ_P) is shown in the insets. The other parameters are $\Delta = 0.001\mu$, $Z = 3$, $\alpha = 0.5$.

and as V is increased from zero, the value of P/I first increases slowly to a maximum value of about $2e$ and then turns to decrease slightly. When $\Delta_S/\Delta_P = 0$, the maximum value of P/I occurs at $V = \Delta/e$. With the increase of Δ_S/Δ_P, the position of the maximum value shifts gradually towards the direction of zero-bias voltage. Overall speaking, the value of P/I is close to $2e$ both in the in-gap region and in the out-gap region for $\Delta_P \geqslant \Delta_S$. In such cases, the electric current is carried mainly by single electrons instead of Cooper pairs even in the in-gap region.

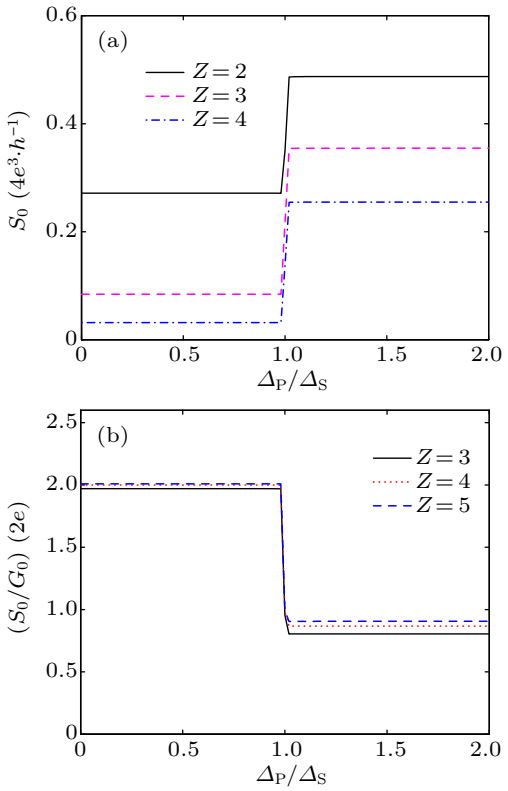


Fig. 3. (a) The variation of the differential shot noise S_0 at zero-bias voltage with the change of the relative amplitude between Δ_P and Δ_S for the barrier strength $Z = 2, 3, 4$. (b) The variation of S_0/G_0 with the change of the relative amplitude between Δ_P and Δ_S for the barrier strength $Z = 3, 4, 5$. The other parameters are: $\Delta = 0.001\mu$, $\alpha = 0.5$.

The results shown in Figs. 1 and 2 indicate that, in the vicinity of zero-bias voltage, both the differential shot noise and the ratio of noise power to electric current may exhibit sharp changes as the relative amplitude between Δ_S and Δ_P is varied from the $\Delta_P < \Delta_S$ regime to the $\Delta_P > \Delta_S$ regime. This fact is more clearly illustrated in Fig. 3. Figure 3(a) shows the change of the differential shot noise S_0 at zero-bias voltage with the variation of Δ_P/Δ_S for the barrier strength $Z = 2$, 3, 4. From Fig. 3(a) we can see that, both in the $\Delta_P < \Delta_S$ regime and in the $\Delta_P > \Delta_S$ regime, the value of S_0 is almost little affected by the variation of the relative amplitude between Δ_P and Δ_S, but in the vicinity of $\Delta_P/\Delta_S = 1$, a sharp increase in the value of S_0 occurs as the relative amplitude between Δ_P and Δ_S is varied from the $\Delta_P < \Delta_S$ regime to the $\Delta_P > \Delta_S$ regime.

In the vicinity of zero-bias voltage, the value of the ratio of noise power to electric current can be given by the value of S_0/G_0, where G_0 is the charge conductivity at zero-bias voltage. Figure 3(b) shows the change of S_0/G_0 with the variation of Δ_P/Δ_S for the barrier strength $Z = 3$, 4, 5. From Fig. 3(b) we can see that, both in the $\Delta_P < \Delta_S$ regime and in the $\Delta_P > \Delta_S$ regime, the value of S_0/G_0 is also little affected by the variation of the relative amplitude between Δ_P and Δ_S, but in the vicinity of $\Delta_P/\Delta_S = 1$, a sharp decrease in the value of S_0/G_0 occurs as the relative amplitude between Δ_P and Δ_S is varied from the $\Delta_P < \Delta_S$ regime to the $\Delta_P > \Delta_S$ regime. Though the value of S_0 may be affected substantially by the variation of the barrier strength (as seen from Fig. 3(a)), the value of S_0/G_0 is only slightly affected by the variation of the barrier strength in both regimes of $\Delta_P < \Delta_S$, and $\Delta_P > \Delta_S$, which is about $4e$ for $\Delta_P < \Delta_S$ and slightly smaller than $2e$ for $\Delta_P > \Delta_S$. From theoretical point of view, such sharp changes are due to two factors. The first is that the effect of the Pauli repulsion becomes much substantial if the triplet component is dominant in the pairing potential. Due to this effect, the electric current will be carried mainly by single electrons instead of Cooper pairs even in the vicinity of zero-bias voltage. The second is that helical Andreev bound state will be formed at the junction interface if $\Delta_P > \Delta_S$, which disappears for $\Delta_P < \Delta_S$. This is a quantum phase transition,[6,16–18] with the critical point $\Delta_P = \Delta_S$.

4. Summary

In summary, we have presented a theoretical investigation on the electrical shot noise properties of tunnel junctions between a normal metal and a superconductor where the mixing of singlet s-wave and chiral triplet p-wave pairing and strong Rashba spin–orbit coupling coexist due to broken inversion symmetry. The variations of the shot noise properties with the changes of the relative amplitude between the two parity components are examined in some detail. It is shown that both the variations of the differential shot noise and the variations of the ratio of noise power to electric current with the bias voltage may exhibit some significantly different features in the different regimes of $\Delta_S > \Delta_P$, $\Delta_S = \Delta_P$, and $\Delta_S < \Delta_P$. In the $\Delta_P \geqslant \Delta_S$ regime, the ratio of noise power to electric current is close to $2e$ both in the in-gap and in the out-gap region. In the $\Delta_S > \Delta_P$ regime, the value of this ratio is close to $4e$ in the inner gap region but may reduce to about $2e$ in the outer gap region as the relative amplitude of the chiral triplet pairing component is increased. The differential shot noise spectrums also exhibit some significant differences in different regimes of the relative amplitude between the two parity components. For instance, on the low bias voltage side of the sharp peak in the differential shot noise spectrum, the variation of the differential shot noise with the bias voltage is monotonic if $\Delta_S > \Delta_P$ but non-monotonic if $\Delta_P > \Delta_S$. The observation of such different features can provide some valuable information on the relative magnitude of the two parity components in the pairing potential. For instance, by measuring the ratio of noise power to electric current in the vicinity of zero-bias voltage, whether the singlet pairing or the triplet pairing component is dominant in the pairing potential can be inferred, and through the analysis of the peak structure in the differential shot noise spectrum, the relative amplitude between the two parity components can be estimated. This would serve as useful diagnostic tools for the determination of the relative magnitude of the two parity components, in complement to usual diagnostic tools based on conductance measurement. Finally, it should be pointed out that the results obtained in the present work are based on a simplified theoretical model where some important effects that may affect the electrical shot noise properties are not included, *e.g.*, the Zeeman effect or the effect of other types of spin–orbit coupling. If the influences of such effects are included in the model, some features of the electrical shot noise properties may be altered substantially. The influences of such effects will be investigated in the future.

References

[1] Tinkham M 1996 *Introduction to Superconductivity* (New York: McGraw-Hill)
[2] Sigrist M and Ueda K 1991 *Rev. Mod. Phys.* **63** 239
[3] Gor'kov L P and Rashba E I 2001 *Phys. Rev. Lett.* **87** 037004
[4] Kimura N, Ito K, Saitoh K, Umeda Y, Aoki H and Terashima T 2005 *Phys. Rev. Lett.* **95** 247004
[5] Wu S T and Yip S 2004 *Phys. Rev. B* **70** 104511
[6] Bauer E and Sigrist M 2012 *Lecture Notes in Physics* (Heidelberg: Springer)
[7] Burset P, Keidel F, Tanaka Y, Nagaosa N and Trauzettel B 2014 *Phys. Rev. B* **90** 085438
[8] Sau J D, Lutchyn R M, Tewari S and Das Sarma S 2010 *Phys. Rev. Lett.* **104** 040502
[9] Alicea J 2010 *Phys. Rev. B* **81** 125318
[10] Lutchyn R M, Sau J D and Das Sarma S 2010 *Phys. Rev. Lett.* **105** 077001
[11] Oreg Y, Refael G and von Oppen F 2010 *Phys. Rev. Lett.* **105** 177002
[12] Stanescu T D, Lutchyn R M and Das Sarma S 2011 *Phys. Rev. B* **84** 144522
[13] Yamakage A, Tanaka Y and Nagaosa N 2012 *Phys. Rev. Lett.* **108** 087003
[14] Potter A C and Lee P A 2011 *Phys. Rev. B* **83** 184520
[15] Mourik V, Zuo K, Frolov S M, Plissard S R, Bakkers E P A M and Kouwenhoven L P 2012 *Science* **336** 1003
[16] Fu L and Kane C L 2008 *Phys. Rev. Lett.* **100** 096407
[17] Hasan M Z and Kane C L 2010 *Rev. Mod. Phys.* **82** 3045
[18] Qi X L and Zhang S C 2011 *Rev. Mod. Phys.* **83** 1057
[19] Asano Y and Tanaka Y 2013 *Phys. Rev. B* **87** 104513
[20] Nadj-Perge S, Drozdov I K, Li J, Chen H, Jeon S, Seo J, MacDonald A H, Bernevig B A and Yazdani A 2014 *Science* **346** 602
[21] Feldman B E, Randeria M T, Li J, Jeon S, Xie Y, Wang Z, Drozdov I K, Andrei Bernevig B and Yazdani A 2017 *Nat. Phys.* **13** 286
[22] Chen J, Woods B D, Yu P, Hocevar M, Car D, Plissard S R, Bakkers E P A M, Stanescu T D and Frolov S M 2019 *Phys. Rev. Lett.* **123** 107703
[23] Elliott S R and Franz M 2015 *Rev. Mod. Phys.* **87** 137

[24] Linder J and Robinson J W A 2015 *Nat. Phys.* **11** 307
[25] Eschrig M 2011 *Physics Today* **64** 43
[26] Tanaka Y, Yokoyama T, Balatsky A V and Nagaosa N 2009 *Phys. Rev. B* **79** 060505
[27] Lu C K and Yip S 2010 *Phys. Rev. B* **82** 104501
[28] Yip S 2014 *Annu. Rev. Condens. Matter Phys.* **5** 15
[29] Romano A, Noce C and Cuoco M 2019 *Phys. Rev. B* **99** 224507
[30] Bøkje K and Sudbø A 2006 *Phys. Rev. B* **74** 054506
[31] Iniotakis C, Hayashi N, Sawa Y, Yokoyama T, May U, Tanaka Y and Sigrist M 2007 *Phys. Rev. B* **76** 012501
[32] Vorontsov A B, Vekhter I and Eschrig M 2008 *Phys. Rev. Lett.* **101** 127003
[33] Fujimoto S 2009 *Phys. Rev. B* **79** 220506
[34] Asano Y and Yamano S 2011 *Phys. Rev. B* **84** 064526
[35] Klam L, Einzel D and Manske D 2009 *Phys. Rev. Lett.* **102** 027004
[36] Yuan H Q, Agterberg D F, Hayashi N, Badica P, Vandervelde D, Togano K, Sigrist M and Salamon M B 2006 *Phys. Rev. Lett.* **97** 017006
[37] Blanter Y M and Büttiker M 2000 *Phys. Rep.* **336** 1
[38] Anantram M P and Datta S 2000 *Phys. Rev. B* **53** 16390
[39] Tanaka Y, Asai T, Yoshida N, Inoue J and Kashiwaya S 2000 *Phys. Rev. B* **61** 11902
[40] Zhu J X and Ting C S 1999 *Phys. Rev. B* **59** 3353
[41] de Jong M J M and Beenakker C W J 1994 *Phys. Rev. B* **49** 16070
[42] Kane C L and Fisher M P A 1994 *Phys. Rev. Lett.* **72** 724
[43] Landauer R 1993 *Phys. Rev. B* **47** 16427
[44] Liu K, Xia K and Bauer G E W 2012 *Phys. Rev. B* **86** 020408
[45] Blonder G E, Tinkham M and Klapwijk T M 1982 *Phys. Rev. B* **25** 4515